

# An Inverse Substrate Orientation for the Regioselective Acylation of 3',5'-Diaminonucleosides Catalyzed by *Candida antarctica* lipase B?

Iván Lavandera,<sup>a,b</sup> Susana Fernández,<sup>a</sup> Julia Magdalena,<sup>a</sup> Miguel Ferrero,<sup>a</sup> Romas J. Kazlauskas,<sup>b,†,\*</sup>  
and Vicente Gotor<sup>a,\*</sup>

<sup>a</sup> Departamento de Química Orgánica e Inorgánica, Facultad de Química, Universidad de Oviedo,  
33071-Oviedo, Spain

<sup>b</sup> Department of Chemistry, McGill University, Montréal, Québec, H3A 3K6, Canada

[rjk@umn.edu](mailto:rjk@umn.edu) or [vgs@fq.uniovi.es](mailto:vgs@fq.uniovi.es)

<sup>†</sup> Current address: Department of Biochemistry, Molecular Biology and Biophysics and The Biotechnology Institute, University of Minnesota, Saint Paul, MN 55108, USA

**Keywords:** biotransformations, enzyme catalysis, molecular modeling, nucleosides, aminolysis.

**Abstract.** *Candida antarctica* lipase B (CAL-B) catalyzes the regioselective acylation of natural thymidine with oxime esters, and also the regioselective acylation of an analog, 3',5'-diamino-3',5'-dideoxythymidine with non-activated esters. In both cases, acylation favors the less hindered 5'-position up to 80-fold over the 3'-position. Computer modeling of phosphonate transition-state analogs for acylation of thymidine suggests that CAL-B favors acylation of the 5'-position because this orientation allows the thymine ring to bind in a hydrophobic pocket and forms stronger key hydrogen bonds as

compared to acylation of the 3'-position. On the other hand, computer modeling of phosphoramidate analogs of the transition states for acylation of either the 3'- or 5'-amino groups in 3',5'-diamino-3',5'-dideoxythymidine shows similar orientations and hydrogen bonds and thus, do not explain the high regioselectivity. However, computer modeling of inverse structures, where the acyl chain binds in the nucleophile pocket and vice versa, does rationalize the observed regioselectivity. The inverse structures fit the 5'-intermediate thymine ring, but not the 3'-intermediate thymine ring, in the hydrophobic pocket and form a weak new hydrogen bond between the carbonyl O-2 of the thymine and the nucleophile amine only for the 5'-intermediate. A water molecule may transfer a proton from the ammonium group to the active site histidine. As a test of this inverse orientation, we compared the acylation of thymine and 3',5'-diamino-3',5'-dideoxythymidine with butyryl acyl donors and with the isosteric methoxyacetyl acyl donors. Both acyl donors reacted at equal rates for thymidine, but the methoxyacetyl acyl donor reacted four times faster than the butyryl acyl donor for 3',5'-diamino-3',5'-dideoxythymidine. This faster rate is consistent with an inverse orientation for 3',5'-diamino-3',5'-dideoxythymidine where the ether oxygen of the methoxyacetyl group can form a similar hydrogen bond to the nucleophilic amine. This combination of modeling and experiments suggests such lipase-catalyzed reactions of apparently close substrate analogs as alcohols and amines may follow different pathways.

## 1. Introduction

Due to the cleanness, simplicity, and efficiency of enzymatic reactions, they are often the best route to complex molecules such as nucleoside analogs,<sup>1</sup> which are drug candidates for several diseases.<sup>2</sup> For example, pyrimidine nucleoside derivatives show antiviral<sup>3</sup> and antitumor<sup>4</sup> activities. Modifications of the sugar moiety are important sources of new compounds with promising chemotherapeutic properties.<sup>5</sup> One sugar modification is the lipase-catalyzed regioselective acylation of natural 2'-deoxy- and ribonucleosides with vinyl<sup>6a</sup> and oxime esters,<sup>6b-g</sup> and 3',5'-diamino-2',3',5'-trideoxynucleosides using non-activated esters.<sup>7</sup> One of the most useful lipases, *Candida antarctica* B (CAL-B), shows high

regioselectivity for the functional group at the ribose 5' position. The molecular basis of this regioselectivity is the focus of this paper.

Lipases, which normally catalyze hydrolysis of lipids, also catalyze the acylation of alcohols as well as amines in organic solvents.<sup>8</sup> Their reaction mechanism involves a Ser-His-Asp (Glu) catalytic triad,<sup>9</sup> where five or six key hydrogen bonds are critical to catalysis. X-Ray structures of transition state analogs as well as molecular modeling show that formation of these hydrogen bonds defines the orientation of the substrate in the active site.<sup>10</sup> The acyl group binds in a large hydrophobic pocket in lipases, while the nucleophile (usually alcohol or amine) binds in a smaller pocket, called a medium hydrophobic pocket. Parts of a large nucleophile may extend into the large hydrophobic pocket or point into the solvent.

However, substantial experimental evidence also suggests that serine hydrolases can tolerate an inverse orientation, where the acyl group binds in the nucleophile site and the nucleophile binds in the acyl group site. One line of evidence is the use of 'inverse substrates' with proteases. For example, trypsin favors hydrolysis peptides with Arg in the acyl portion of the substrate, but also catalyzes hydrolysis of esters of *p*-amidinophenol or 4-guanidinophenol, where the arginine side chain mimic is in the alcohol moiety (Chart 1).<sup>11</sup> Bordusa and coworkers exploited this inverse substrate idea to overcome the narrow substrate specificity of trypsin.<sup>12</sup> Instead of accepting only peptides with Arg in the acyl portion, trypsin accepted a wide range of acyl groups when Bordusa and coworkers used esters of 4-guanidinophenol. They suggest that the broadened substrate range stems from the inverse orientation, which places the 4-guanidinophenyl group in the amidino-moiety-requiring acyl group site and the diverse acyl groups in the less structurally demanding nucleophile-binding site.<sup>13</sup> Recently, this group extended the same idea to clostripain,<sup>14</sup> which has a similar specificity to trypsin, and also to the Glu-specific V8 protease.<sup>15</sup> Another line of evidence for inverse binding of substrates comes from the inhibition of acetylcholine esterase with P-chiral methylphosphonates (nerve agents). Both enantiomers inhibit this enzyme, but, due to the different configuration at phosphorus, bind differently. The slow-reacting enantiomer binds in the inverse orientation.<sup>16</sup> Inhibition of lipases by carbamates may also

involve such a reverse binding.<sup>17</sup> Finally, the X-ray crystal structure of CAL-B containing a phosphonate transition state analog unexpectedly showed an inverse orientation.<sup>18</sup> Thus, there is a strong evidence that transition-state analogs can bind in an inverse orientation and that substrates can both bind and react in an inverse orientation.

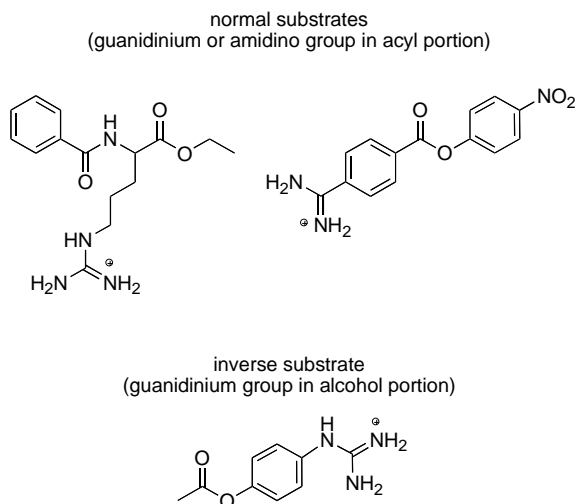


**Chart 1.** Normal and inverse ester substrates for trypsin. Normal ester substrates for trypsin contain a guanidinium or amidino group in the acyl portion. However, trypsin also accepts esters of 4-guanidinophenol, where the guanidinium moiety is in the alcohol moiety. The most likely explanation is that the ester reacts in an inverse orientation.

Although the use of enzymes in synthesis is common, the basis of their selectivity is not well understood. The goal of this study is to identify the molecular basis of the 5'-regioselectivity of CAL-B toward nucleosides and their analogs using computer modeling. This modeling suggests that the acylation of natural nucleosides favors the 5'-position because this orientation allows the thymine base to bind in a large hydrophobic pocket. On the other hand, modeling suggests that acylation of diamionucleosides proceeds via an inverted substrate orientation and regioselectivity stems from better binding of the thymine ring when the 5'-amino group reacts and from a stabilizing interaction between the *O*-2 carbonyl group of the base and the 5'-amine nucleophile.

## 2. Results

### 2.1. Regioselective CAL-B-Catalyzed Acylation of Thymidine

Previous work reported CAL-B-catalyzed acylations of nucleosides with good 5'-selectivity using oxime esters as the acyl donor and tetrahydrofuran (THF) as the solvent (Scheme 1, X= O).<sup>6b-g</sup> The selectivity was similar for adenine, thymidine, guanine and cytidine,<sup>6</sup> so we focused on the simplest one – thymidine – for this study. We tested five acetonoxime esters as acylating agents: three with an aliphatic acyl chain (R= Me, Pr, Non) and two with acyl chains containing aromatic rings (R= Ph, CH<sub>2</sub>Ph) (Table 1). We used dry THF as the solvent because previous work showed that the regioselectivity was highest in this solvent.<sup>19</sup>

**Scheme 1.** Regioselective CAL-B-catalyzed acylation of thymidine (**1**) and 3',5'-diamino-3',5'-dideoxythymidine (**2**) (T= thymine).

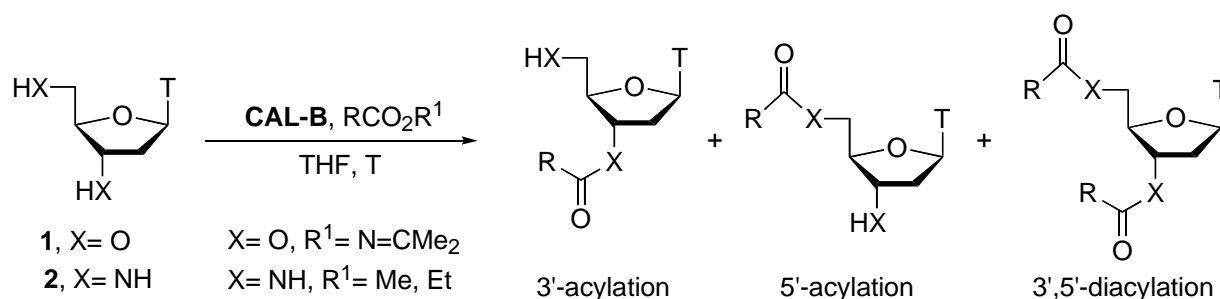


**Table 1.** Regioselectivity of CAL-B catalyzed acylation of thymidine (**1**) with oxime esters.<sup>a</sup>

Entry	acyl group	R	T (°C)	<i>t</i> (h) <sup>b</sup>	conv (%)	3' (%)	5' (%)	3',5' (%)	5' selectivity <sup>c</sup>
1	acetyl	Me	30	4	98	17	68	13	2.7:1
2	butanoyl	Pr	30	6.5	94	11	81	2	6.4:1
3	decanoyl	Non	30	53.5	99	20	79	0	4:1
4	benzoyl	Ph	30	39	12	0	12	0	>12:1
5	benzoyl	Ph	60	30	41	1	40	0	40:1
6	phenylacetyl	Bn	30	37	45	0	45	0	>45:1

7	phenylacetyl	Bn	60	6	75	0	75	0	>75:1
---	--------------	----	----	---	----	---	----	---	-------

<sup>a</sup> Reactions were monitored by gas chromatography, except for the acetylation reaction. In this case, peaks of the acetylation products overlapped on GC chromatograms, so the reactions were monitored by HPLC. <sup>b</sup> Time refers to either the time to reach high conversions or the time where no further reaction was observed. <sup>c</sup> Selectivity was estimated from the ratio of the 3' and 5' monoacylated products plus the amount of double acylation added to each.

For the oxime esters with aliphatic acyl chains the regioselectivities were moderate (2.7:1 for acetyl, 6.4:1 for butanoyl and 4:1 for decanoyl; entries 1–3, Table 1). The acylation was complete in 4 to 6.5 h for acetyl and butanoyl, respectively, but required 53.5 h for decanoyl. For the oxime esters with an aromatic ring in the acyl chain, the regioselectivity was higher (>12:1 and >45:1), but the rate was very slow at 30 °C (entries 4 and 6, 12–45% conversion after 37–39 h, Table 1). At 60 °C, the regioselectivity remained high (40:1 and >75:1) and the conversions increased to 41% and 75% for benzoyl and phenylacetyl, respectively, in shorter reaction times (entries 5 and 7, 6–30 h, Table 1).

## 2.2. Molecular Modeling of the CAL-B-Catalyzed Acylation of Thymidine

To explain the regioselectivities of CAL-B for the 5'-OH of thymidine, we used computer modeling starting from an X-ray crystal structure of CAL-B. We modeled phosphonate analogs of the transition state for butanoylation of thymidine at both the 5' and 3' positions. The starting point for modeling was a simple phosphonate, which mimics the transition state for butanoylation of ethanol (Figure 1, R= *n*-C<sub>3</sub>H<sub>7</sub>).<sup>18</sup> Geometry optimization of this simple phosphonate formed all six essential hydrogen bonds for catalysis. To model the nucleoside substrates, we added the ribose and thymidine rings and systematically searched for catalytically productive conformations (see Supporting Information). We defined catalytically productive conformations as those that: a) contained all six key catalytic hydrogen bonds, b) avoided steric clashes between the phosphonate and the lipase, and c) avoided steric clashes within the phosphonate.

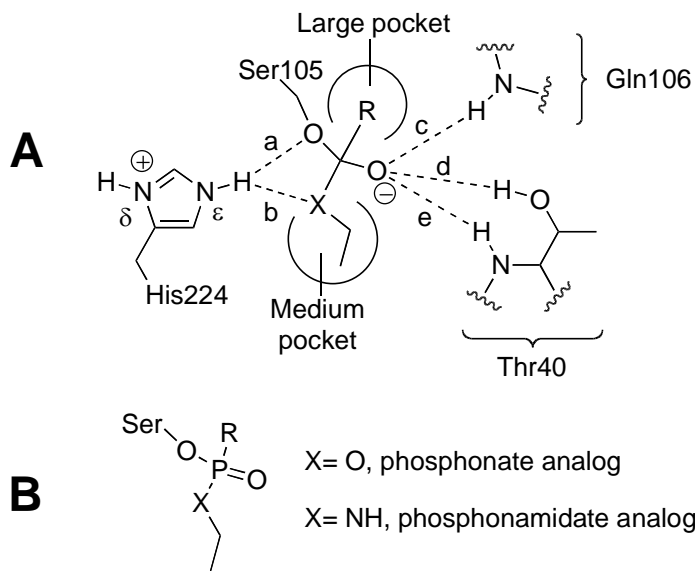


**Figure 1.** Tetrahedral intermediates for the acylation of ethanol (X= O) or ethylamine (X= NH) in the normal orientation and the corresponding phosphonate (X= O) or phosphoramidate (X= NH) transition state analogs. A) Key hydrogen bonds between CAL-B and the tetrahedral intermediate are: two from  $N_{\delta}$  of His224 to the oxygen of Ser105 and the XEt group of the tetrahedral intermediate (X= O, NH), and three from the oxyanion to Gln106 (one) and to Thr40 (two). A sixth key hydrogen bond is from  $N_{\delta}$  of His224 to the carboxylate of Asp187 (not shown). B) A phosphonate (X= O) or phosphoramidate (X= NH) analogs mimicked these tetrahedral intermediates in computer modeling. Further, the XEt groups are replaced by either the 5'- or 3'-nucleoside in a stepwise fashion as described in the text.

The active site of CAL-B restricts the possible orientations for the nucleoside (Figure 2).<sup>20</sup> Viewed with the catalytic triad Asp-His-Ser oriented from left to right, it contains a large hydrophobic pocket above the Asp-His-Ser triad and a medium size pocket below it. In the normal orientation, the acyl moiety of the substrate lies in the large hydrophobic pocket, while the alcohol (nucleophile) moiety lies in the medium pocket, but may extend into the solvent and/or into the large hydrophobic pocket. The large hydrophobic pocket in CAL-B is lined by Ile189 and Val190 on the left, Val154 on the far right, as well as Leu140 and Leu144 at the top of the pocket. Deep in this pocket, Asp134 is on the left and Gln157 on the right. The medium pocket is below the catalytic Ser105 and is crowded by Trp104 below

it and the Leu278-Ala287 helix to the right. It has little room for substituents larger than propyl; several carbons of the bound nucleoside lie in this region, but most of the nucleoside extends out into solvent or into the large hydrophobic pocket (see below).

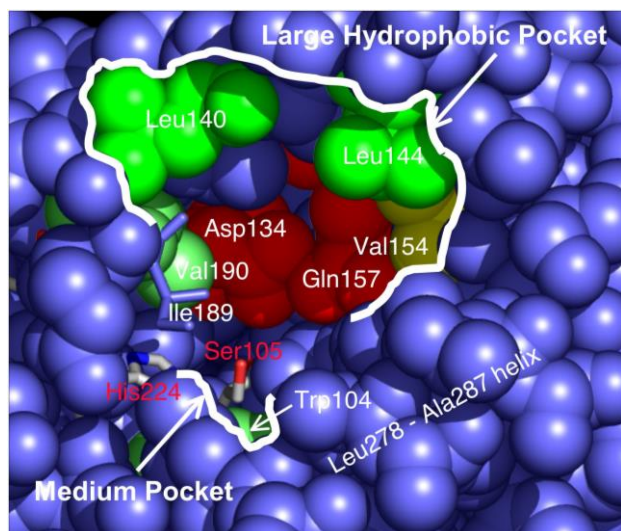


**Figure 2.** CAL-B active site structure from X-ray crystallography viewed with the catalytic triad Asp-His-Ser oriented from left to right (Asp187 is hidden). The acyl group of the substrate binds first in the large hydrophobic pocket. This usually situates the substrate with the acyl group above the catalytic triad and the leaving group, or the nucleophile, below the catalytic triad. The active site contains a large hydrophobic pocket above the catalytic residues and a medium sized pocket below. There is very little room for large substituents below the active site of CAL-B. The above image displays Ile189 in a stick representation to allow a better view of the large pocket of the lipase.

#### *5' butanoylation catalyzed by CAL-B (favored)*

The best model of the tetrahedral intermediate for the 5'-*O*-butanoylation (Figure 3A),<sup>21</sup> orients the thymine in the right side of the large hydrophobic pocket above Gln157, with all six key hydrogen bonds and no intra- or intermolecular steric clashes (entry 1, Table 2).



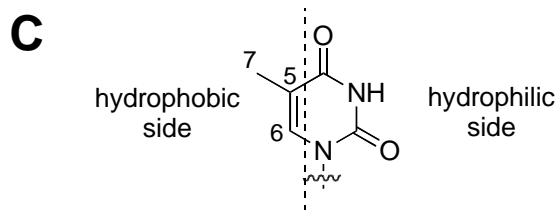
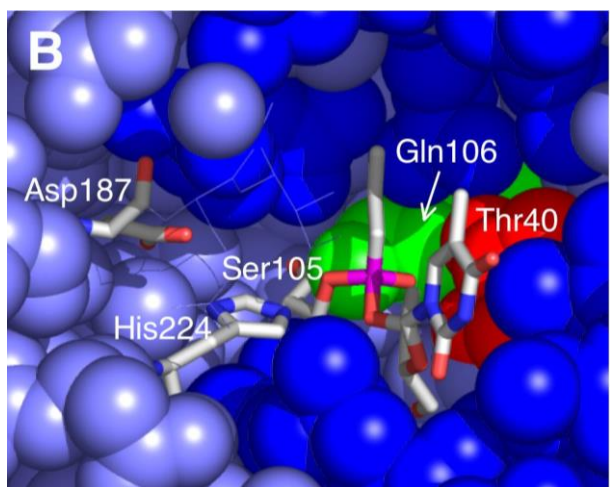
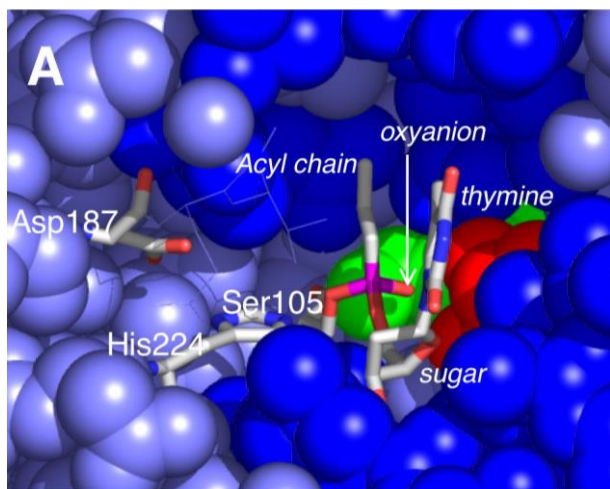


**Figure 3.** The best conformations of 5'- (A) and 3'-butyrylated (B) intermediates of thymidine in CAL-B are shown above, and also the hydrophobic and hydrophilic moieties of thymine ring (C). The tetrahedral intermediate for the favored 5' acylation reaction (A) situates the thymine ring on the right side of the large hydrophobic pocket, making it the most productive conformation due to better enzyme substrate interaction. The tetrahedral intermediate for the 3' acylation reaction (B) situates the thymine ring outside the hydrophobic pocket. The binding thymine ring appears to be the key factor to explain the enzyme regioselectivity. Darker spheres indicate the amino acids that are the limits of the medium

and large hydrophobic size pockets around the CAL-B active site (see Figure 2). The above image displays Glu188 and Ile189 in a line representation to allow a better view of the large pocket of the lipase.

**Table 2.** Key hydrogen bond angles and distances in CAL-B-catalyzed acylation of thymidine and 3',5'-diaminothymidine.

Entry	Figure <sup>a</sup>	H-bond distance, Å (angle) <sup>b</sup>				
		a	b	c	d	e
1	3A	3.05 (124°)	3.08 (164°)	2.92 (157°)	2.75 (166°)	2.87 (172°)
2	3B	3.17 (131°)	2.87 (159°)	3.11 (163°)	2.78 (159°)	2.74 (164°)
3	S2	2.91 (153°)	3.25 (125°)	3.27 (160°)	2.77 (163°)	2.88 (157°)
4	S3	3.23 (141°)	3.14 (144°)	3.14 (160°)	2.75 (164°)	2.74 (159°)
5	6A <sup>c</sup>	- <sup>d</sup>	- <sup>d</sup>	3.14 (160°)	2.76 (152°)	2.73 (148°)
6	S4	- <sup>d</sup>	- <sup>d</sup>	3.22 (161°)	2.78 (151°)	2.77 (112°)
7	7 <sup>e</sup>	- <sup>d</sup>	- <sup>d</sup>	3.11 (159°)	2.75 (152°)	2.75 (150°)
8	S5 <sup>c</sup>	- <sup>d</sup>	- <sup>d</sup>	3.06 (163°)	2.79 (152°)	2.70 (145°)
9	6C <sup>f</sup>	- <sup>d</sup>	- <sup>d</sup>	3.09 (163°)	2.77 (152°)	2.71 (147°)

<sup>a</sup> See the text. <sup>b</sup> Figure 1 defines the hydrogen bonds. Distances are between non-hydrogen atoms (N-N, N-O, O-O), and angles refer to the N-H-O or similar. <sup>c</sup> In these Figures appear a new short distance between the carbonyl O-2 of the thymine and the N-5' nucleophile. Figure 6A: 3.36 Å (126°); Figure S5: 3.13 Å (111°). <sup>d</sup> Not relevant due to inverse orientation of substrate, since distances are more than 4 Å. <sup>e</sup> Distance between the carbonyl O-2 of the thymine and the N-5' nucleophile: 3.41 Å (127°); distance between the water oxygen and the N-5' nucleophile: 4.13 Å (111°); distance between the water oxygen and the N<sub>ε</sub>-Histidine: 5.28 Å. <sup>f</sup> Distance between the carbonyl O-2 of the thymine and the N-5' nucleophile: 3.14 Å (118°); distance between the methoxyacetyl oxygen and the N-5' nucleophile: 2.54 Å (100°); distance between the methoxyacetyl oxygen and the N<sub>ε</sub>-Histidine: 3.21 Å.

The hydrophobic side of the thymine ring (C-5 – C-7) lies close to other hydrophobic groups (Figure 3C): the side chains of Val154, Ile189 and Ile285 and the propyl group of the acyl portion. Thus, the C-6 of the thymine ring is 3.94 Å far away from the C-α of the acyl chain, the C-5 is 5.42 Å from the C-β,

and the *C*-7 (methyl group of thymine) is 4.08 Å from the *C*-γ. The hydrophilic side of the thymine ring points toward the solvent, but also lies near the hydrophobic methyl group of Ala282.

*3' butanoylation catalyzed by CAL-B (not favored)*

The *trans* orientation of the 3' alcohol and thymine prevents placing the thymine ring in the large pocket and extends it beyond the medium pocket, preventing binding there as well. The best structure has the thymine ring lying partly on the protein surface having some van der Waals contacts with the enzyme (entry 2, Table 2; Figure 3B). In this conformation, the thymine ring lies on the lower right edge of the large hydrophobic pocket with the hydrophobic side of the thymine ring near the side chains of Ile189 and Ile285. The 5'-OH of this structure rested in the small area below the catalytic Ser105, between His224, Trp104 and Leu278. In addition to the inability to bind the thymine ring in the hydrophobic pocket, this structure contains two destabilizing interactions. First, the hydrophilic side of thymine lies near the hydrophobic side chains of Ala282 and Leu278 and *O*-2 of thymidine is near the carbonyl oxygen of Leu278. Second, it lacks a hydrophobic interaction between the propyl acyl chain and the hydrophobic side of the thymine [the *C*-6 of the thymine ring is 5.19 Å away from the acyl chain *C*-α, *C*-5 is 7.43 Å from the *C*-β, and *C*-7 (methyl group of thymine) is 6.83 Å from the *C*-γ]. These distances are 1.3–2.8 Å longer than those for the 5'-intermediate. Thus, binding of the thymine ring in the large pocket during acylation at the 5'-position is the most likely molecular basis for the high regioselectivity of CAL-B for the 5'-position.

The interaction of the thymine ring with the acyl chain may be the origin of the altered regioselectivity with different acylating agents. An acetyl group would show a smaller interaction than a butanoyl group and indeed the regioselectivity is lower for acetylation as compared to butanoylation (2.7 vs. 6.4; Entries 1 and 2, Table 1). For decanoylation the regioselectivity was lower than for butanoylation (4.0 vs. 6.4; Entries 3 and 2, Table 1), but the hydrophobic side of thymine is much smaller than a decanoyl group and cannot interact with the entire chain. In addition, the larger decanoyl group may crowd the large

hydrophobic pocket. The phenyl or benzyl acyl group may make additional  $\pi$ -stacking interactions with thymidine and thereby show higher regioselectivity (40 or >75; Entries 5 and 7, Table 1).

### 2.3. Regioselective CAL-B-Catalyzed Acylation of 3',5'-Diaminothymidine

CAL-B shows even higher regioselectivity in the acylation of the thymidine analog, 3',5'-diamino-3',5'-dideoxythymidine (**2**, Scheme 1, X= NH).<sup>7b</sup> For example, acetylation of thymidine showed only a 2.7:1 regioselectivity for the 5'-position (entry 1, Table 1), while acetylation of the amino analog showed a 17:1 regioselectivity for the 5'-position (entry 1, Table 3). Similarly the regioselectivity for butanoylation increased from 6.4:1 to >68:1 (compare entry 2, Table 1 and entry 3, Table 3). To avoid chemical acylation, we used unactivated esters as acyl donors and added molecular sieves (4 Å), which accelerated these acylations (Table 3).<sup>22</sup> Varying the concentration of acylating agent did not change the regioselectivity. For the butanoyl, crotonoyl and phenyl moieties, regioselectivity remained high towards the 5'-position. For the formylation and acetylation reactions, we always observed mixtures between 5'-acylated and 3',5'-diacylated compounds in ratios depending on the reaction time.

**Table 3.** Regioselectivity of CAL-B-catalyzed acylation of 3',5'-diaminothymidine (**2**) with non-activated esters.<sup>a</sup>

Entry	Acyl group	R <sup>b</sup>	R <sup>1b</sup>	T (°C)	t (h) <sup>c</sup>	5' (%)	3', 5' (%)	5' selectivity <sup>d</sup>
1	acetyl	Me	Et	40	6	80	5	17:1
2	formyl	H	Et	40	8	55	20	3.8:1
3	butanoyl	Pr	Et	40	32	68	0	>68:1
4	crotonoyl	MeCH=CH	Me	60	31	83	0	>83:1
5	benzoyl	Ph	Me	60	75	67	0	>67:1

<sup>a</sup> See Ref. 7b. <sup>b</sup> See Scheme 1. <sup>c</sup> Time refers to either the time to reach high conversions or the time where no further reaction was observed. <sup>d</sup> Selectivity was estimated from the ratio of the 3' and 5' monoacylated products plus the amount of double acylation added to each.

## 2.4. Molecular Modeling of the CAL-B-Catalyzed Acylation of 3',5'-Diaminothymidine

### 2.4.1. Molecular modeling of the normal orientation

Modeling of the CAL-B-catalyzed acetylation of 3',5'-diamino-3',5'-dideoxythymidine (**2**, Scheme 1) started with a geometry optimization of the corresponding phosphoramidates,<sup>23</sup> Figure 1B (X= NH, R= CH<sub>3</sub>) (Supporting Information, Figure S2 and Figure S3). However, in spite of the similarity of phosphonates and phosphoramidates, the phosphoramidate structures showed longer distances for key hydrogen bonds a–c (Entries 3 and 4, Table 2).<sup>24</sup> In the 5'-intermediate, the longer hydrogen bonds were those between catalytic His and nucleophile (3.25 Å) and between oxyanion and Gln106 (3.27 Å). In the 3'-intermediate, the longer hydrogen bond was between His224 and Ser105 (3.23 Å). Thus, modeling cannot explain the experimentally observed strong preference for the 5'-position.

The origin of these differences in the phosphonate and phosphoramidate structures is likely the lower electronegativity of the NH vs. O as well as subtle differences in the bond lengths and bond angles in the two structures [P-O bond lengths (1.62 Å) vs. P-N (1.54 Å)]. Due to the rigidity of the intermediates, these small differences in bond lengths and angles can make larger differences in the orientation of the substrate (an 'arc effect'). Furthermore, the lower electronegativity of the nitrogen weakens the hydrogen bond between His224 and the NH of the nucleoside, and the hydrogen of the nucleophile is placed close to His224, the catalytic histidine (Figure 4).

Two additional destabilizing interactions in the 5'-acetylation intermediate may decrease the difference between the 5'- and 3'-acetylation intermediates. The 5'-acetylation intermediate lacks the hydrophobic interaction between the hydrophobic side of the thymine and the acyl group because this ring does not bind as deeply into the large hydrophobic pocket. Second, the 5'-acetylation intermediate places the polar 3'-NH<sub>2</sub> near the hydrophobic side chains of Ala281, Leu278, and Trp104 in the medium size pocket.

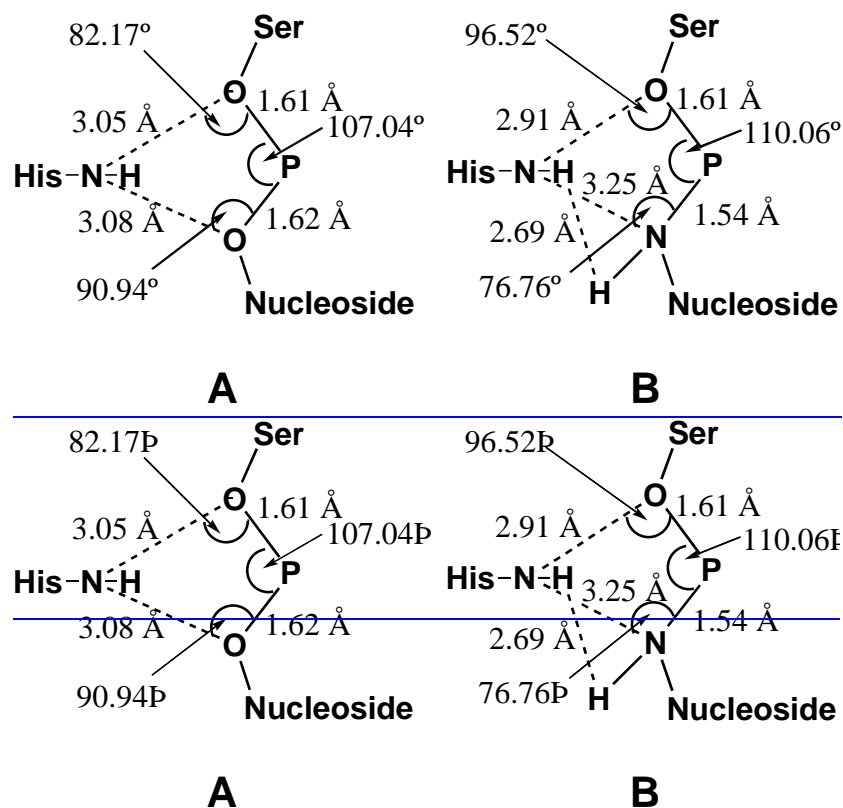


**Figure 4.** Comparison of the bond angles and lengths in phosphonate vs. phosphoramidate transition state analogs. A) Structure for the 5'-acylation of thymidine (Figure 3A) shows a symmetrical structure while; B) intermediate for the 5'-acetylation of 3',5'-diaminonucleoside (Figure S2) shows longer P-O than P-N bond lengths. The lower electronegativity of the nitrogen weakens the hydrogen bond between His224 and the NH of the nucleoside (3.25 Å). Furthermore, the hydrogen of the nucleophile is placed close to His224, the catalytic histidine.

#### 2.4.2. Inverse mechanism: overall fit

Since normal orientation models did not explain the increased regioselectivity with the same acylating agents we considered an inverse orientation, where the acyl chain fits in the medium hydrophobic pocket, and the diaminonucleoside nucleophile fits in acyl-binding region of the large pocket (Figure 5). Initially, we focused on the transition state for acylation of the aminonucleoside to test the overall fit of the inverse orientation. This acylation could occur for the aminolysis reaction without the assistance of the catalytic histidine because amines are much more nucleophilic than alcohols. Furthermore, the minor steric hindrance of the diaminonucleoside in the large hydrophobic pocket could favor these structures.

Thus for example, in the inverse structure (Figure 6A) there are several destabilizing interactions between the nucleoside and three amino acids (Gln157, Ile189, and Ile285) around 4 Å from nucleoside; meanwhile, with the normal orientation (Figure S2), seven amino acids destabilize the intermediate at that distance (Thr40, Trp104, His224, Leu278, Ala281, Ala282, and Ile285).

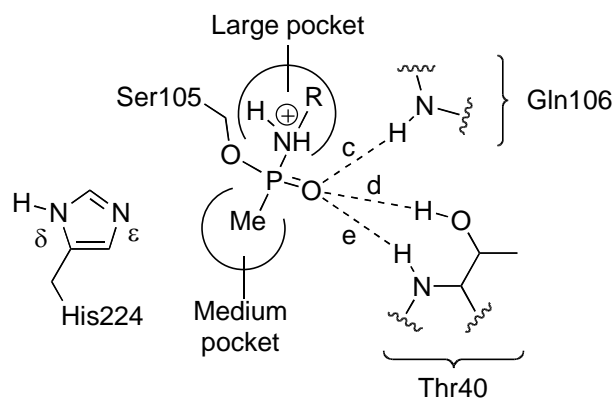


**Figure 5.** Inverse orientation of the phosphonamidate transition state analog for acylation of 3',5'-diaminopyrimidine from the active site of CAL-B. The 3',5'-diaminopyrimidine ( $R-NH_2^+$  moiety) lies in the large hydrophobic pocket and the methyl group binds in the medium pocket.

#### *5' acetylation catalyzed by CAL-B (favored)*

The best model of the tetrahedral intermediate for the 5'-*N*-acetylation, Figure 6A, shows the sugar and the thymine moieties in the large hydrophobic pocket with *C*-4, and *N*-3 pointing out to the solvent. Four of the six key hydrogen bonds were present while avoiding inter- and intramolecular steric interactions (entry 5, Table 2). The methyl group of the acetate bound on the medium pocket. An interaction between the *O*-2 carbonyl group of the base and the 5'-amine nucleophile (3.36 Å) may also stabilize this structure (Figure 6B).

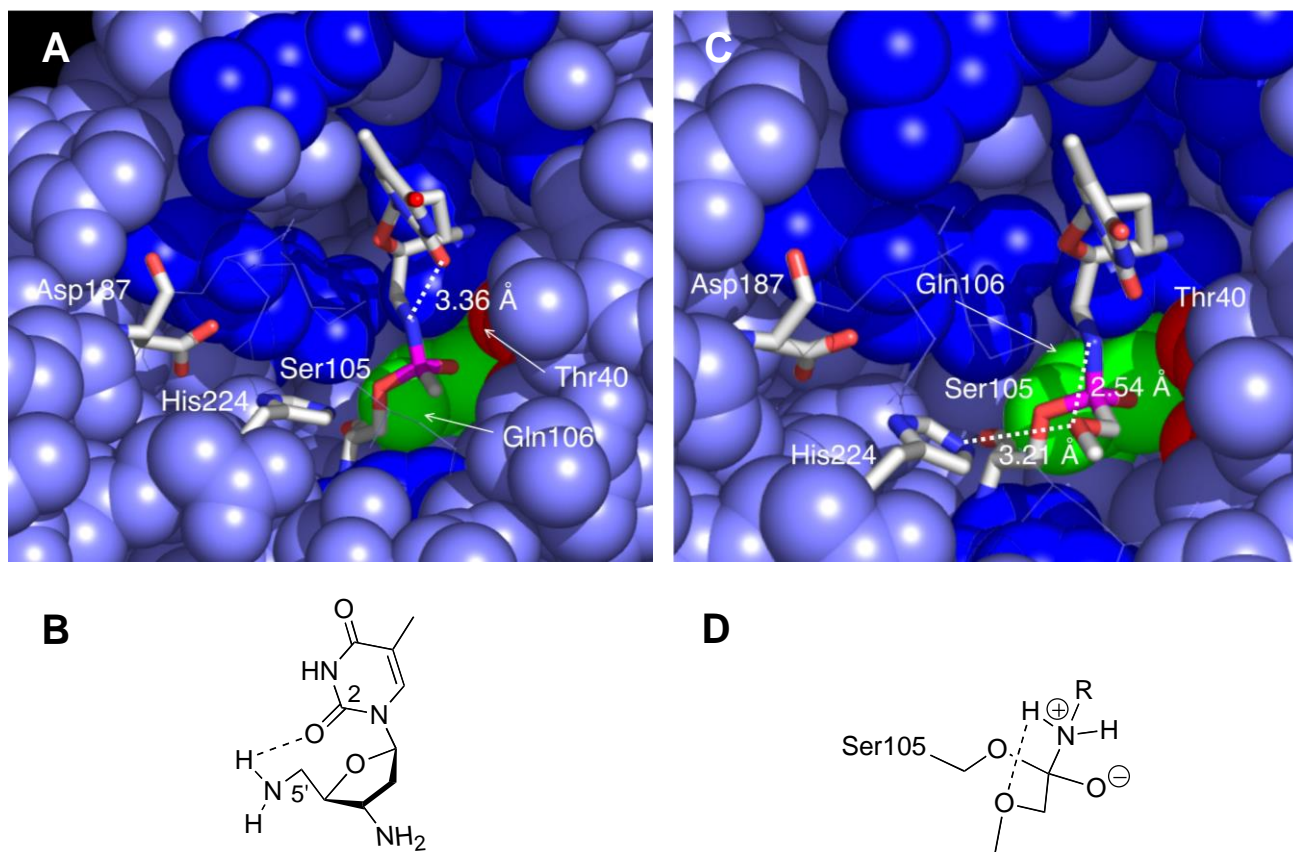


**Figure 6.** A) Best model of phosphoramidate for *N*-5'-acetylated intermediate of **2** in the inverse conformation. This tetrahedral intermediate situates the sugar ring and thymine in the large hydrophobic pocket. A potential hydrogen bond stabilization appears between the *O*-2 carbonyl group of thymine and the nucleophilic 5'-amino group nitrogen; B) Detail of the hydrogen bond between the *O*-2 of the thymine ring and the 5'-NH<sub>2</sub> nucleophile; C) Best model of the amine-protonated intermediate of **2** and the methoxymethyl group with CAL-B in the inverse conformation. The methoxymethyl chain places the oxygen atom between the ammonium group and the N<sub>ε</sub>-histidine, making possible the transference of the proton autocatalyzed; D) Possible stabilizing interaction of the methoxymethylene acyl chain in the protonated amine intermediate for the aminolysis.

*3'* acetylation catalyzed by CAL-B (not favored)



In this intermediate, the sugar placed in the large hydrophobic pocket, but the thymine ring did not bind into this subsite and pointed out to the solvent (Figure S4 available in Supporting Information). No structures were found to fit the thymine ring in a hydrophobic region of the catalytic site.

These models for acetylation of the nucleoside could explain the high regioselectivity of CAL-B for acylation of the 5'-amino group. The loss of one of the key hydrogen bonds, in the 3'-phosphoramidate, between the oxyanion and Thr40 (angle  $<120^\circ$ , entry 6, bond e, Table 2), and better binding of the thymine ring in the 5'-intermediate appear to be key determinant of the lipase selectivity. Also, the 3'-acylation intermediate lacks an interaction between the O-2 carbonyl and the nucleophile amine due to its *trans* orientation.

#### **2.4.3. Inverse mechanism: proton transfers**

The modeling above showed that the shape of the active site allows an inverse orientation. However, these structures contained only four of the six key hydrogen bonds for catalysis. The role of the missing hydrogen bonds is to transfer a proton from the nucleophile (amine) to the serine. To be plausible as catalytically productive structures, the inverse orientation must provide an alternate path for these proton transfers. Thus, initial attack of the amino nucleoside on the acyl enzyme intermediate leads to a protonated species, which we mimic as a phosphoramidate ( $\text{P-NH}_2^+-\text{R}$ ). In the normal mechanism, the catalytic histidine transfers the proton from the initially protonated species to serine, but this histidine is too far away from the nucleophile in the inverse orientation to allow a direct proton transfer (3.71 Å to  $\text{N}_\epsilon$  of His224). Direct transfer of the proton from the ammonium group to the oxygen of the serine is also unlikely due to an acute angle ( $\text{N-H-O} = 68^\circ$ ).<sup>24</sup> Modeling suggests that a water molecule may aid a stepwise proton transfer.

Previously, modeling suggested that an alcohol could transport a proton between the substrate and the key histidine in the CAL-B catalyzed enantioselective ring opening of  $\beta$ -lactams.<sup>25</sup> In our case, water could play this role, since water remains bound to the lipase even in organic solvents. We modelled a

water molecule in several positions near the catalytic triad and found a stable position midway between the protonated amine and the histidine in these inverse phosphoramidate intermediates (Figure 7). The water molecule is about 4 Å from the ammonium group and 5 Å from the N<sub>ε</sub>-histidine. This position is still too far to hydrogen bond with either group, but small movements of this water would allow stepwise proton transfer from the ammonium moiety to the N<sub>ε</sub> of His224 (entry 7, Table 2).

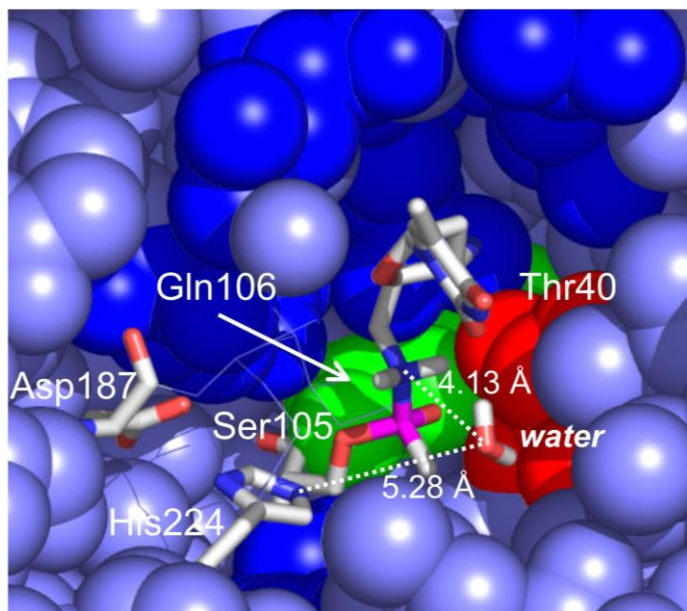


**Figure 7.** Best model of the *N*-5'-inverse intermediate of **2** stabilized with a water molecule. This molecule places almost equidistant from the nucleophile amine and the His224. In this structure the water molecule does not form a hydrogen bond with the protonated amine, but small motions of this water molecule would allow stepwise transfer from the amino group to the histidine or serine. Residues Glu188 and Ile189 are shown in lines for clarity.

Furthermore, the carbonyl *O*-2 was close to the 5'-amino group nitrogen (3.41 Å), making the latter more nucleophile. This interaction has a potential catalytic role since it could replace the activation effect on the amino group due to the N<sub>ε</sub> of His224 in the serine mechanism and could be a key reason for the excellent regioselectivity of the lipase. This interaction may also be involved in the proton transfer from the ammonium group to the histidine or serine.

#### 2.4.4. Kinetic evidence for an inverse mechanism

A key feature of the proposed inverse mechanism is an interaction between the 5'-NH<sub>2</sub> group and the O-2 carbonyl of the thymine, which makes that position more nucleophilic. As further evidence for the importance of the interaction between the 5'-NH<sub>2</sub> group and the O-2 carbonyl of the thymine, we note that diamionucleosides containing this O-2 carbonyl [thymidine, 2'-deoxyuridine, (*E*)-5-(2-bromovinyl)-2'-deoxyuridine] undergo *N*-acylation,<sup>7</sup> while a compound that lacks this O-2 carbonyl (*N*-benzoyl-2'-deoxyadenosine) does not. However, CAL-B does catalyze the acylation of the corresponding natural purine nucleoside even though it does not contain this O-2 carbonyl group.<sup>6c-d</sup> This difference further suggests that the acylation of alcohols and amines may follow different pathways.

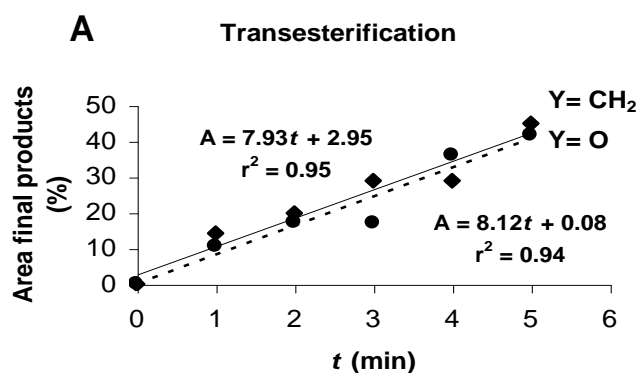
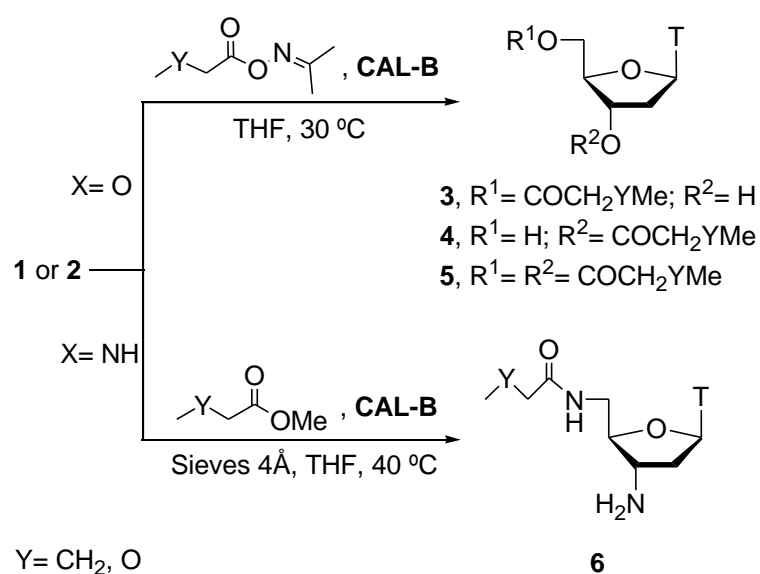
The faster enzymatic aminolysis reactions with methoxyacetate esters as compared to the isosteric butyryl esters<sup>26</sup> is one key to the successful commercialization of a lipase-catalyzed kinetic resolution of amines.<sup>27</sup> Although the inductive effect of the β-oxygen to the carbonyl group may contribute to the faster reaction, this explanation is inconsistent with the lack of a similar faster acylation of alcohols.

To the best of our knowledge, there is no explanation for this effect based on the normal orientation of substrates in the active site. However, we hypothesized that the β-oxygen could accelerate the reaction of amines if they reacted via an inverse mechanism (Figure 6D). To test this hypothesis, we compared the rates of acylation of nucleoside alcohols and amines using acyl donors with and without a β-oxygen. We predicted that acyl donors containing a β-oxygen should react faster than those without a β-oxygen in the acylation of amines because they follow the inverse mechanism, but not in the acylation of alcohols because they follow the normal mechanism.

We first compared the initial rates of the CAL-B-catalyzed esterification of natural nucleoside **1** (Scheme 2). We used oximes as the acyl donors because they showed the fastest rates and best yields in previous work.<sup>6b-g</sup> Short reaction times yielded only 5'-acylated (**3**) and 3'-acylated (**4**) products but longer reaction times also yielded 3',5'-diacylated nucleosides (**5**). Both initial rates were similar (slope = 7.9 vs. 8.1) indicating no significant influence by the β-oxygen in the acyl chain (Figure 8A). Second,

we compared the initial rates of the CAL-B aminolysis of **2** (Scheme 2). We used methyl esters as acyl donors because the oximes also reacted without lipase catalysis.<sup>7</sup> These acylations yielded only 5'-monoacylated nucleosides (**6**). The initial rates differed approximately four-fold (slope = 1.4 vs. 4.9) indicated a faster reaction for the acyl donor with a  $\beta$ -oxygen in the acyl chain (Figure 8B).<sup>28</sup> This result is consistent with the amine nucleoside **2**, but not natural nucleoside **1**, reacting via an inverse mechanism.

**Scheme 2.** Regioselective enzymatic acylation of **1** using oxime esters and **2** with methyl esters.



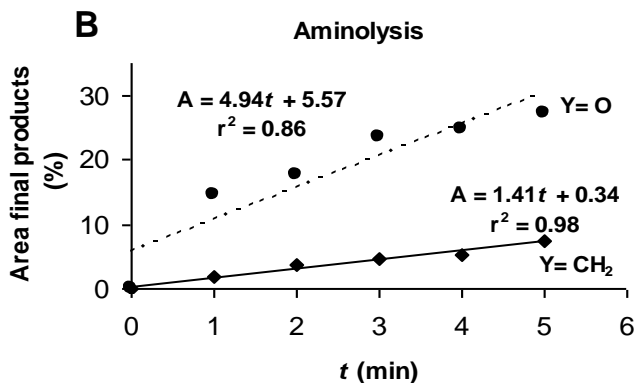


**Figure 8.** Initial rates of CAL-B catalyzed processes: A) enzymatic transesterification reactions of **1** with oxime butyrate (filled line) and oxime methoxyacetate (dotted line) show similar initial rates for both acylating agents; B) enzymatic aminolysis reactions of **2** with methyl butyrate (filled line) and methyl methoxyacetate (dotted line) show an approximately four-fold faster initial rate for methyl methoxyacetate, consistent with a possible catalytic role of this  $\beta$ -oxygen in the acylation of amines.

Molecular modeling supports the suggestion that the  $\beta$ -oxygen has a catalytic role in the acylation of aminonucleoside **2** via an inverse mechanism. Modeling of the acylation of **2** with a propyl group via an inverse mechanism following the same approach outlined above for acetylation yielded similar structures (Figure S5 available in Supporting Information). The diamionucleoside fits in the large hydrophobic pocket, while the propyl group fits in the medium subsite. However, modeling of the acylation with the methoxyacetyl group following an inverse mechanism revealed a potential catalytic role of the  $\beta$ -oxygen (Figure 6C). The oxygen of the acyl moiety lay close to both the ammonium group (2.54 Å), stabilizing its positive charge, and close to N $\epsilon$  of the His224 (3.21 Å). This location is ideal to act as a proton transporter.<sup>29</sup>

### 3. Discussion

CAL-B shows excellent regioselectivity for the acylation of natural<sup>6</sup> and non-natural<sup>7</sup> nucleosides towards the chemically more reactive 5'-position. The enzyme active site structure influences this

regioselectivity. For example, CAL-B was the only biocatalyst that showed high regioselectivity of the 5'-position in 3',5'-diaminonucleosides, while the lipase from *Pseudomonas cepacia* (PSL-C) favored the 3'-position.<sup>7b</sup> The regioselectivity for aminolysis was much higher than for transesterification (Tables 1 and 3 and Section 2.4.4).

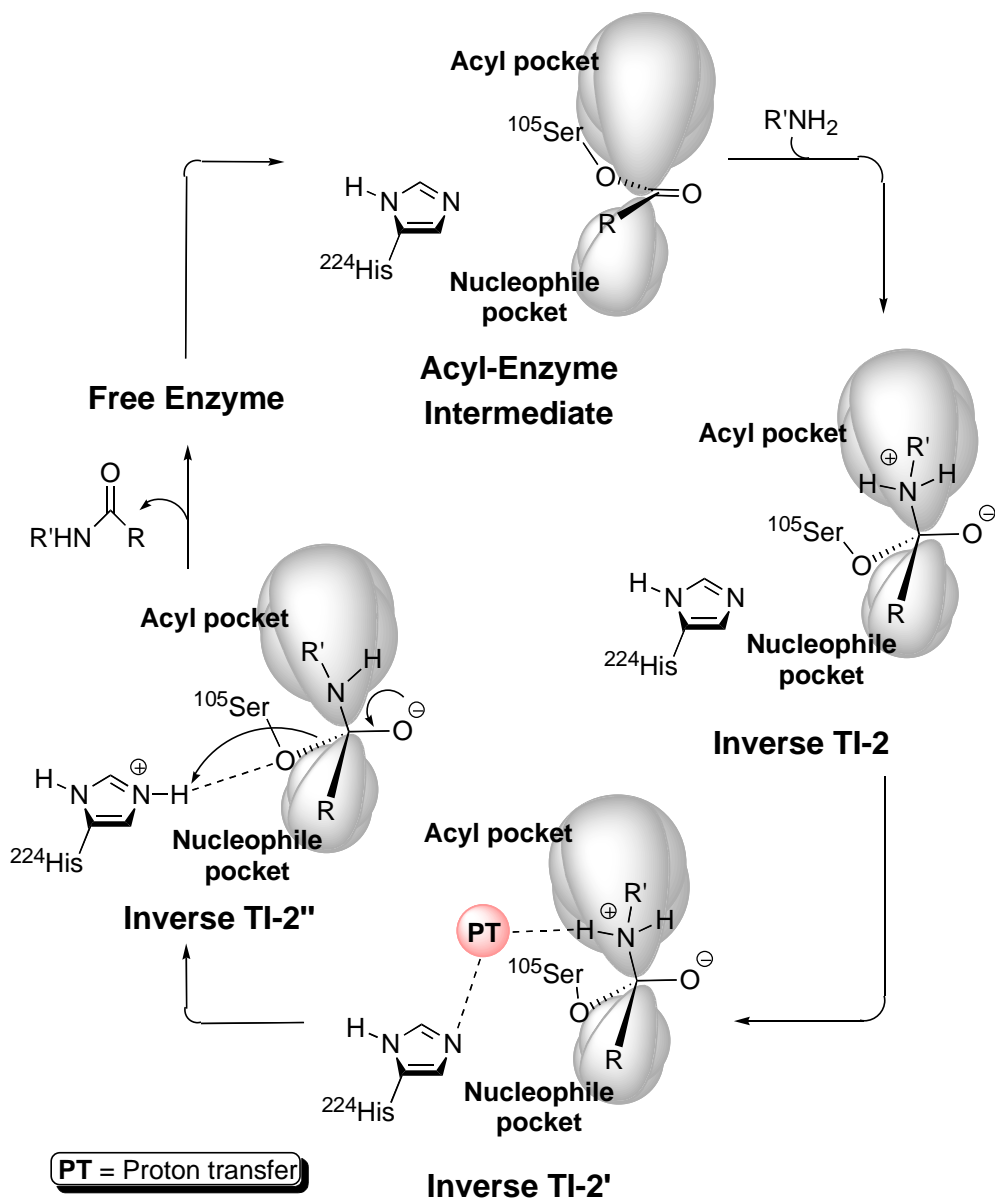
For the natural nucleosides (acylation of an alcohol moiety), molecular modeling identified a molecular basis for the observed regioselectivity. Acylation of the 5'-OH binds the thymine base in a hydrophobic pocket, while acylation of the 3'-OH does not. An interaction between the acyl chain and the thymine ring may explain why regioselectivity varies with different acyl groups.

For the 3',5'-diaminonucleosides, modeling of a normal orientation did not explain the preference for the 5'-NH<sub>2</sub> because in the 5'-intermediate several stabilizing interactions were lost and similar orientations and hydrogen bonds are present in both 3'- and 5'-structures. To explain the observed regioselectivity in 3',5'-diaminonucleosides, we considered an inverse orientation, which has an opposite binding of the nucleophile and the acyl chain in the active site of the lipase. Bordusa and coworkers proposed an inverse orientation in several protease-catalyzed reactions, but this is the first proposal of an inverse disposition in lipase-catalyzed reactions. Modeling this inverse orientation easily explained the observed regioselectivity. First, the structure for acylation at the slower-reacting 3'-position showed a poorer fit of the thymine ring in the hydrophobic pocket and lacked a key hydrogen bond. On the other hand, the structure for acylation at the faster reacting structure 5'-position showed a new stabilizing interaction between the carbonyl O-2 of the thymine and the nucleophile amine, which may have a catalytic role.

In spite of the higher nucleophilicity of amines compared to alcohols, most hydrolase-catalyzed acylations involve alcohols not amines. Further, reactions with amines are often slower, requiring larger amounts of hydrolase or longer reaction times. In this paper, we suggest a possible reason for this difference for the specific case of the CAL-B-catalyzed regioselective acylation of natural nucleosides and 3',5'-diaminonucleosides. Scheme 3 summarizes the proposed inverse mechanism for the aminolysis reaction with CAL-B. Although we have no direct evidence for the proposed mechanism, we

have indirect kinetic evidence together with modeling. We also have no direct or indirect evidence that would rule out this mechanism. The key difference occurs in the second tetrahedral intermediate (TI-2). The amine (nucleophile) attacks directly without histidine activation, creating a zwitterionic structure where the ammonium group binds into the large hydrophobic pocket, placing the ester chain in the medium subsite (inverse TI-2). Later, a proton transfer (e.g. molecule of water), carries a proton from the ammonium group to the histidine residue (inverse TI-2'), and finally, the subsequent intermediate (inverse TI-2'') would evolve as usual transferring the proton to the oxygen of the serine yielding the corresponding amide.

**Scheme 3.** Inverse mechanism for enzymatic aminolysis reaction with CAL-B.



This reaction via an inverse orientation is an example of catalytic promiscuity.<sup>30</sup> This term means the ability of enzyme active sites to catalyze distinct chemical transformations which may differ in the functional group involved, that is, the type of bond formed or cleaved during the reaction and/or in the catalytic mechanism or path of bond making and breaking. CAL-B has already demonstrated that is able to catalyze other type of reactions, such as aldol<sup>31</sup> or Michael additions.<sup>32</sup> The inverse substrate orientation proposed in this paper is an example of a different catalytic mechanism for CAL-B. Bocola *et al.*<sup>33</sup> have previously described the X-ray structure of CAL-B phosphoramidate bound to both



enantiomers of 1-phenylethylamine showing normal orientation, but other X-ray structures for phosphonates showed an inverse orientation.<sup>16,18</sup>

Other examples of altered catalytic mechanism include: a) reactions after removal of a catalytically essential amino acid residue, which dramatically slow reactions, but do not eliminate them. The remaining less efficient reaction must follow a different path,<sup>34</sup> b) reactions that involve substrate-assisted catalysis, where the only substrates converted are those that restore the missing functional group so that it can actively participate in catalysis;<sup>35</sup> and c) reactions catalyzed by binding proteins from no bond breaking to some bond breaking. For example, bovine serum albumin catalyzes several types of transformations,<sup>36</sup> myoglobin performs slow oxidations in the presence of hydrogen peroxide,<sup>37</sup> and in several cases, a catalytic antibody created to catalyze one reaction can also promote another reaction.<sup>38</sup>

## 4. Experimental Section

**4.1. General.** *Candida antarctica* lipase B (CAL-B, Novozym 435, 7300 PLU/g) was a gift from Novo Nordisk Co. All other reagents were purchased from commercial sources. THF was dry over sodium metal and pyridine over potassium hydroxide and then were distilled under nitrogen atmosphere.

**4.2. Molecular Modeling.** The program Insight II, version 2000.1, was used for viewing the structures. The geometric optimizations were performed using Discover, version 2.9.7 (*Accelrys*, San Diego CA, USA), using the AMBER<sup>39</sup> force field. The distance dependent dielectric constant was set to 4.0 to mimic the electrostatic shielding of the solvent and the 1-4 van der Waals interactions were scaled to 50%. The crystal structure for the CAL-B (1lbs<sup>18</sup>) was obtained from the Protein Data Bank ([www.rcsb.org/pdb/](http://www.rcsb.org/pdb/)), and includes a phosphonate. Protein structures in Figures 2, 3, 6, and 7 were generated using PyMOL 0.97.

**4.3. Initial Rates of Esterification Reactions.** A solution containing the oxime ester (0.5 mmol), and **1** (48 mg, 0.2 mmol) in THF (2 mL) was prepared in an Erlenmeyer flask. This mixture was introduced in an orbital shaker (250 rpm), and allowed to stand for at least 30 min at 30 °C. Finally, CAL-B (50 mg) was added to the solution, and at regular intervals of 1 min, a 100 µL sample was extracted from the

flask (five samples per reaction), the solvent was evaporated, and the sample was silylated. The sample was analyzed by gas chromatography (GC) on a TRACSIL TRB-5A capillary column (30 m × 0.32 mm × 0.50 μm), with nitrogen as carrier gas and a flame ionization detector. Injector and detector temperatures were set at 300 °C, head column pressure at 14 psi and split 90:1, column initial temperature 220 °C (3 min), rate 5 °C/min until 260 °C, then 15 min at 260 °C, followed by heating rate 5 °C/min until 300 °C, column final temperature was 300 °C (10 min). 3',5'-Di-*O*-TMS-2'-deoxyuridine (as internal standard) appeared at 11.8 min; 5'-*O*-Butyryl-3'-*O*-TMS-thymidine<sup>6f</sup> at 15.9 min; 3'-*O*-butyryl-5'-*O*-TMS-thymidine<sup>6g</sup> at 16.3 min; 3',5'-di-*O*-butyrylthymidine<sup>6f</sup> at 23.1 min; 5'-*O*-methoxyacetyl-3'-*O*-TMS-thymidine at 16.8 min; 3'-*O*-methoxyacetyl-5'-*O*-TMS-thymidine at 17.3 min; 3',5'-di-*O*-methoxyacetylthymidine at 26.8 min. Standard curves were produced enabling the concentration of the ester product to be followed over time. The spectroscopical data of 5'-*O*-, 3'-*O*-, and 3',5'-di-*O*-methoxyacetylthymidine are collected in the Supplementary Information.

**4.4. Initial Rates of Aminolysis Reactions.** A solution containing the methyl ester (0.67 mmol), 3',5'-diamino-3',5'-dideoxythymidine (**2**) (20 mg, 0.08 mmol), and molecular sieves 4Å (20 mg) in THF (4.5 mL) was prepared in an Erlenmeyer flask. This mixture was introduced in an orbital shaker (250 rpm), and allowed to stand for at least 30 min at 40 °C. Finally, CAL-B (10 mg) was added to the solution, and at regular intervals of 1 min, a 100 μL sample was extracted from the flask (five samples per reaction), and the solvent was evaporated. Then, the samples were analyzed by high performance liquid chromatography (HPLC) on a Kromasil 100 C18 column (150 × 4.6 mm, 5 μm). HPLC conditions: constant flow: 0.5 mL/min; temperature: 25 °C; eluent gradient: A:B 1:99 (6 min), then polarity was changed linealy until A:B 20:80 at 15 min, and finally was changed linealy until A:B 100:0 at 25 min, where A: CH<sub>3</sub>CN, and B: ammonium acetate 0.02M with contains 1% CH<sub>3</sub>CN. 3',5'-Diamino-3',5'-dideoxythymidine<sup>7b,40</sup> at 4.2 and 7.0 min; 3'-amino-5'-butyrylamino-3',5'-dideoxythymidine<sup>7b</sup> at 18.7 min; 3'-amino-5'-methoxyacetylamino-3',5'-dideoxythymidine (spectroscopical data is collected in the Supplementary Information) at 16.6 min.

**Acknowledgments.** We express our appreciation to Novo Nordisk Co. for the generous gift of the CAL-B. Financial support of this work by the Spanish Ministerio de Ciencia y Tecnología (Project PPQ-2001-2683) and by Principado de Asturias (Project GE-EXP01-03) is gratefully acknowledged. S.F. thanks MCYT for a personal grant (Ramón y Cajal Project). I.L. and J.M. thank MCYT for pre-doctoral fellowships.

**Supporting Information Available.** Molecular modeling details and experimental procedures are described. Complete  $^1\text{H}$ ,  $^{13}\text{C}$ , and DEPT NMR spectral data and some 2D NMR experiments are shown in addition to mp, IR, microanalysis, optical rotation, and MS data. The level of purity is indicated by the inclusion of copies of  $^1\text{H}$  and  $^{13}\text{C}$  NMR spectra. Furthermore, some extensive modeling figures are included. This material is available free of charge via the Internet at <http://www.chembiochem.org>.

## References

1. (a) M. Ferrero, V. Gotor, *Chem. Rev.* **2000**, *100*, 4319-4347. (b) M. Ferrero, V. Gotor, *Monatsh. Chem.* **2000**, *131*, 585-616.
2. (a) C. M. Galmarini, *Electron. J. Oncol.* **2002**, *1*, 22-32. (b) R. K. Robins, G. R. Revankar, In *Antiviral Drug Development*; E. De Clercq, R. T. Walker, Eds.; Plenum Press: New York, 1998; p 11. (c) T. K. Mansour, R. Storer, *Curr. Pharm. Res.* **1997**, *3*, 227-264.
3. (a) S. Czernecki, J. M. Valery, In *Carbohydrates in Drug Design*; Z. J. Witczak, K. A. Nieforth, Eds.; Dekker: New York, 1997; p 495. (b) E. De Clercq, *Pyrimidine Nucleoside Analogs as Antiviral Agents*; NATO ASI Series, Series A: Life Sciences **1984**, *73*, 203-230.
4. W. Plunkett, V. Gandhi, *Cancer Chemother. Biol. Response Modif. Annu.* **2001**, *19*, 21-45.
5. E. T. Kool, *Chem. Rev.* **1997**, *97*, 1473-1487.

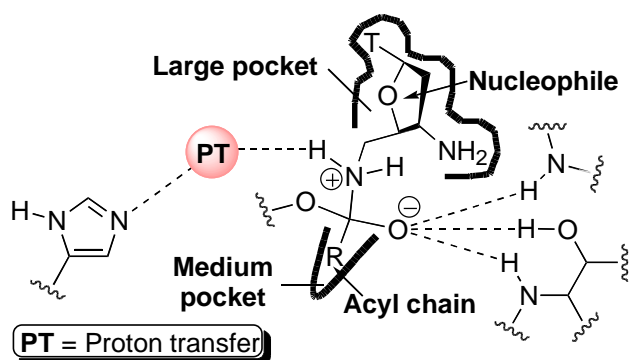
6. (a) J. García, S. Fernández, M. Ferrero, Y. S. Sanghvi, V. Gotor, *Tetrahedron Lett.* **2004**, *45*, 1709-1712. (b) J. García, S. Fernández, M. Ferrero, Y. S. Sanghvi, V. Gotor, *Org. Lett.* **2004**, *6*, 3759-3762. (c) J. García, S. Fernández, M. Ferrero, Y. S. Sanghvi, V. Gotor, *Tetrahedron: Asymmetry* **2003**, *14*, 3533-3540. (d) J. García, S. Fernández, M. Ferrero, Y. S. Sanghvi, V. Gotor, *Nucleosides Nucleotides Nucleic Acids* **2003**, *22*, 1455-1457. (e) F. Morís, V. Gotor, *Tetrahedron* **1993**, *49*, 10089-10098. (f) F. Morís, V. Gotor, *J. Org. Chem.* **1993**, *58*, 653-660. (g) V. Gotor, F. Morís, *Synthesis* **1992**, 626-628.
7. (a) I. Lavandera, S. Fernández, M. Ferrero, E. De Clercq, V. Gotor, *Nucleosides Nucleotides Nucleic Acids* **2003**, *22*, 1939-1952. (b) I. Lavandera, S. Fernández, M. Ferrero, V. Gotor, *J. Org. Chem.* **2001**, *66*, 4079-4082.
8. U. T. Bornscheuer, R. J. Kazlauskas, *Hydrolases in Organic Synthesis*; Weinheim: Wiley-VCH, 1999.
9. (a) L. Hedstrom, *Chem. Rev.* **2002**, *102*, 4501-4523. (b) A. R. Fersht, *Enzyme Structure and Mechanism*, 2nd Ed.; Freeman: Nueva York, 1985.
10. (a) W. V. Tuomi, R. J. Kazlauskas, *J. Org. Chem.* **1999**, *64*, 2638-2647. (b) J. Zuegg, H. Höning, J. D. Schrag, M. Cygler, *J. Mol. Cat. B* **1997**, *3*, 83-98. (c) M. Cygler, P. Grochulski, R. J. Kazlauskas, J. D. Schrag, F. Bouthillier, B. Rubin, A. N. Serreqi, A. K. Gupta, *J. Am. Chem. Soc.* **1994**, *116*, 3180-3186.
11. K. Tanizawa, Y. Kanaoka, W. B. Lawson, *Acc. Chem. Res.* **1987**, *20*, 337-343.
12. F. Bordusa, D. Ullmann, C. Elsner, H.-D. Jakubke, *Angew. Chem. Intl. Ed. Engl.* **1997**, *36*, 2473-2475.
13. M. Thormann, S. Thust, H.-J. Hofmann, F. Bordusa, *Biochemistry* **1999**, *38*, 6056-6062.
14. R. Günther, A. Stein, F. Bordusa, *J. Org. Chem.* **2000**, *65*, 1672-1679.

15. N. Wehofsky, F. Bordusa, *FEBS Lett.* **1999**, *443*, 220-224.
16. C. Luo, H. Leader, Z. Radic, D. M. Maxwell, P. Taylor, B. P. Doctor, A. Saxena, *Biochem. Pharm.* **2003**, *66*, 387-392.
17. H.-C. Shin, D. M. Quinn, *Biochemistry* **1992**, *31*, 811-818.
18. J. Uppenberg, N. Öhrner, M. Norin, K. Hult, G. J. Kleywegt, S. Patkar, V. Waagen, T. Anthonsen, T. A. Jones, *Biochemistry* **1995**, *34*, 16838-16851.
19. (a) L. F. García-Alles, V. Gotor, *Biotechnol. Bioeng.* **1998**, *59*, 163-170. (b) L. F. García-Alles, V. Gotor, *Biotechnol. Bioeng.* **1998**, *59*, 684-694.
20. J. Uppenberg, M. T. Hansen, S. Patkar, T. A. Jones, *Structure (London)* **1994**, *2*, 293-308.
21. We obtained 4-6 structures for each regioisomer by systematic search of dihedral angles shown in Figure S1 (see Supporting Information), making changes of 30°. From these structures, we chose the one with the lowest energy that kept all the six key hydrogen bonds. This best intermediate was geometry optimized with further systematic search of dihedral angle of approximately 10–20°.
22. An explanation for this effect: I. Lavandera, S. Fernández, M. Ferrero, V. Gotor, *Tetrahedron* **2003**, *59*, 5449-5456.
23. The IUPAC name of these derivatives is: methyl(alkylamido)phosphonate.
24. To identify hydrogen bonds, a donor atom to acceptor atom distance of less than 3.20 Å and a donor atom - hydrogen - acceptor atom angle of 120° or greater are required.
25. S. Park, E. Forró, H. Grewal, F. Fülöp, R. J. Kazlauskas, *Adv. Synth. Catal.* **2003**, *345*, 986-995.
26. (a) J. González-Sabín, V. Gotor, F. Rebolledo, *Tetrahedron: Asymmetry* **2004**, *15*, 481-488. (b) F. Balkenhohl, K. Ditrich, B. Hauer, W. Ladner, *J. Prakt. Chem.* **1997**, *339*, 381-384.

27. F. Balkenhohl, B. Hauer, W. Ladner, U. Pressler, US 5728876, 1996.
28. Synthesis of the 5'-methoxyacetylamino derivative was also much faster (2 h) than the 5'-butyrylated derivative (32 h).
29. There are studies in which the proton is transferred from a protonated nucleophile amine through substrate-assisted: N. Díaz, D. Suárez, T. L. Sordo, R. Méndez, J. M. Villacorta, *Eur. J. Org. Chem.* **2003**, 4161-4172.
30. U. T. Bornscheuer, R. J. Kazlauskas, *Angew. Chem. Intl. Ed.* **2004**, *43*, 6032-6040.
31. C. Branneby, P. Carlqvist, A. Magnusson, K. Hult, T. Brinck, P. Berglund, *J. Am. Chem. Soc.* **2003**, *125*, 874-875.
32. O. Torre, I. Alfonso, V. Gotor, *Chem. Commun.* **2004**, 1724-1725.
33. M. Bocola, M. T. Stubbs, C. Sotriffer, B. Hauer, T. Friedrich, K. Dittrich, G. Klebe, *Protein Eng.* **2003**, *16*, 319-322.
34. Y. Romsicki, G. Scapin, V. Beaulieu-Audy, S. Patel, J. W. Becker, B. P. Kennedy, E. Asante-Appiah, *J. Biol. Chem.* **2003**, *278*, 29009-29015.
35. A. Magnusson, K. Hult, M. Holmquist, *J. Am. Chem. Soc.* **2001**, *123*, 4354-4355.
36. (a) S. Colonna, N. Gaggero, J. Drabowicz, P. Lyzwa, M. Mikołajczyk, *Chem. Commun.* **1999**, 1787-1788; (b) G. Klein, J.-L. Reymond, *Bioorg. Med. Chem. Lett.* **1998**, *8*, 1113-1116; (c) F. Hollfelder, A. J. Kirby, D. S. Tawfik, *Nature* **1996**, *383*, 60-62.
37. D. C. Levinger, J.-A. Stevenson, L.-L. Wong, *J. Chem. Soc., Chem. Commun.* **1995**, 2305-2306.
38. (a) A. C. Backes, K. Hotta, D. Hilvert, *Helv. Chim. Acta* **2003**, *86*, 1167-1174; (b) L. C. James, D. S. Tawfik, *Prot. Sci.* **2001**, *10*, 2600-2607.

39. (a) W. D. Cornell, P. Cieplak, C. I. Bayly, P. A. Kollmann, *J. Am. Chem. Soc.* **1993**, *115*, 9620-9631. (b) S. J. Weiner, P. A. Kollman, D. A. Case, U. C. Singh, C. Ghio, G. Alagona, S. Profeta, P. Weiner, *J. Am. Chem. Soc.* **1984**, *106*, 765-784.
40. T.-S. Lin, W. H. Prusoff, *J. Med. Chem.* **1978**, *21*, 109-112.

## Table of Contents



**Inverse substrate orientation in lipases:** Hydrolase-catalyzed reactions with amines are often slower than related with alcohols, in spite of the higher nucleophilicity of amino groups. A combination of molecular modeling and kinetic experiments suggests that lipase-mediated processes of apparently close substrate analogs as alcohols and amines may follow different pathway. Thus, regioselective acylation of 3',5'-diamino-3',5'-dideoxythymidine has been rationalized modeling inverse intermediates.